Pressure and Heat-Transfer Investigation of a Hypersonic Configuration

David E. Reubush*
NASA Langley Research Center, Hampton, Virginia
and
M. Emmett Omar†
Boeing Advanced Systems, Seattle, Washington

An investigation was conducted in the Langley 8-Ft High Temperature Tunnel to obtain hypersonic pressure and heat-transfer data on a large scale (1/20) model of a hypersonic wing-body configuration. The model was tested at a nominal Mach number of 6; at two Reynolds numbers (0.6 and 1.6×10^6/ft); and at angles of attack from about 0 to about 15 deg. Results from this investigation indicate that both pressure and heat-transfer coefficients on the windward side of the configuration increased with increasing angle of attack; that leeside heat-transfer coefficients remained relatively constant at slightly below the 0-deg level for all angles of attack; and that leeside pressure coefficients decreased slightly with increasing angle of attack but remained relatively close to a value of 0.

Nomenclature

$b/2$ = wing half span (10.2 in.)
C_p = pressure coefficient, $(p-p_\infty)/q_\infty$
L = length of configuration (78.0 in.)
p = local static pressure, psi
p_∞ = freestream static pressure, psi
$\dot{q}$ = heat-transfer rate (Btu/ft^2-s)
q_∞ = freestream dynamic pressure, psi
$\dot{q}_0$ = stagnation point heat transfer (model scale) for a 1-ft, full-scale hemisphere (Btu/ft^2-s)
Re = Reynolds number
s = local axial distance from wing leading edge, in.
x = axial distance measured from Model Station 0.0, in.
y = lateral distance measured from model centerline, in.
α = model angle of attack, deg
ϕ = circumferential coordinate, deg (0 deg is top of model)

Introduction

In order to achieve the goal of developing a new class of air-breathing hypersonic vehicles, there must be significant advances achieved in a number of disciplines, not the least of which is the development of accurate computational techniques for the prediction of the heat and pressure loads that the vehicle will be subjected to during the portions of the flight trajectory that cannot be duplicated in ground based facilities. As a part of the research efforts to validate advanced computational techniques, an investigation was conducted in the NASA Langley 8-Ft High Temperature Tunnel (8′HTT) with a large scale (1/20) model of a hypersonic wing-body configuration. The purpose of the test series was to obtain pressure and heat-transfer data on a realistic configuration for both laminar and turbulent boundary-layer conditions. In particular, the distribution of the pressure and heat-transfer instrumentation was biased toward the upper surface or leeside of the vehicle (for positive angles of attack) because the prediction of leeside characteristics are significantly more difficult than those for the windward side.

The tests were conducted in the NASA Langley 8′HTT at a nominal Mach number of 6. The unit Reynolds number was varied from about 0.6×10^6 to about 1.6×10^6/ft. The model was tested at angles of attack from about 0 to about 15 deg. Presented are heat-transfer data obtained for 3 rays (0, 90, and 180 deg) on the fuselage and for the upper surface of the wing. Pressure data obtained for 4 rays (0, 30, 90, and 180 deg) on the fuselage are also presented. In addition, a comparison of windward fuselage pressures with predictions from modified Newtonian theory are presented.

Experimental Methods

Wind Tunnel and Tests

The tests were conducted in the NASA Langley 8′HTT. This tunnel is a large-scale, open-throat, blow-down facility that utilizes the combustion products of methane and air as a test medium. The combustion products are expanded through a conical/contoured nozzle with an exit diameter of 8 ft to achieve true temperature simulation of flight at altitudes from 80,000 to 130,000 ft. The tunnel Mach number varies from about 5.8 to 7.3 depending on the particular conditions in the combustor due to losses in the nozzle resulting from the condensation of the water vapor in the test medium. The 5500 psia air storage currently in use for the tunnel allows run times of up to 2 min.

For this particular test series, the combustor pressure was varied from about 1000 psia to about 2500 psia and the combustor temperature was held at about 3200°R. The unit Reynolds number varied from about 0.6×10^6/ft at the low combustor pressure condition to about 1.6×10^6/ft at the high combustor pressure condition. The Mach number varied from

Presented as Paper 89-0246 at the AIAA 27th Aerospace Sciences Meeting, Reno, NV, Jan. 9–12, 1989; received April 29, 1989; revision received Oct. 23, 1989.

*Technical Assistant to the Director for Structures. Member AIAA.
†Senior Engineer.

about 6.5 at the low combustor pressure condition down to about 6.0 at the high combustor pressure condition (at which most data were obtained). Angle of attack was varied from about 0 to about 15 deg. Further description of the NASA Langley 8′HTT and the combustion products test medium can be found in Refs. 1-3.

Model and Support System

This investigation was conducted with a 1/20th scale model of a representative hypersonic wing-body configuration. The nose of the model was a slightly blunted (0.075 in. radius) ogive with an initial half angle of about 9 deg. The ogival nose faired into a circular fuselage with a radius of 3.05 in. at model station 37.8 in. The simulated inlet ramp system was installed starting at model station 50.0 in. with a half width of 5.9 in. The compression side of the ramp system had an angle of 8 deg to the model centerline, and the expansion side had an angle of 11 deg. The model was mounted inverted on the support system so that the model did not significantly increase flow blockage over that resulting from the tunnel support strut when the angle of attack was increased. A sketch of the model is shown in Fig. 1.

The model was instrumented with 96 pressure orifices connected to three 32 port electrically scanned pressure sensor modules (0–5 psi), 24 thin-film, heat-transfer gauges, and 28 Gardon-type calorimeters. The thin-film, heat-transfer gauges were (except for the two in the nose) in groups of six gauges mounted on a block of Macor (only two gauges active) and were utilized in areas of generally lower anticipated heat transfer or areas where there was not the depth necessary for the Gardon-type calorimeters. The Gardon-type calorimeters were generally used in areas of higher anticipated heat transfer and were in two ranges: 0–15 Btu/ft^2-s and 0–60 Btu/ft^2-s. Figure 1 indicates the locations of the various instrumentation.

The model was tested both with and without boundary-layer trips (generally with). The trips were 4- 40 set screws (0.112 in. diam) that were installed in a ring around the nose 4.5 in. aft of the tip and in rows on both upper and lower surfaces of the wing 1.5 in. aft of the leading edge. The trips were installed with a spacing of 4 diam and with a height of 1 diam for the nose and 1/2 diam for the wings.

Procedure

To alleviate start-up loads on the model and to maintain a cold-wall condition, the model was stored below the test section on a hydraulic elevator. After the desired flow conditions were established in the test section, the model was inserted into the stream (in about 2 s) at the desired angle of attack for that particular run. Because the model was constructed primarily of aluminum with stainless-steel nose and wing leading edges, the length of time the model could be in the stream was limited to less than 10 s. Most data were taken at the rate of 20 frames/s beginning before the tunnel start, continuing through model insertion, time in the stream, retraction, and tunnel shutdown. The pressure data were obtained using electrically scanned pressure sensor modules and were taken at a rate of approximately 200 frames/s with the total amount of data being limited by data system memory to only 5 s. The acquisition of these data was started as the model was being inserted and continued until the data system memory was full. An average of the first 2 s of data taken after the model was inserted and the angle of attack had stabilized are presented as the most representative of that for a cold-wall condition at the desired angle of attack.

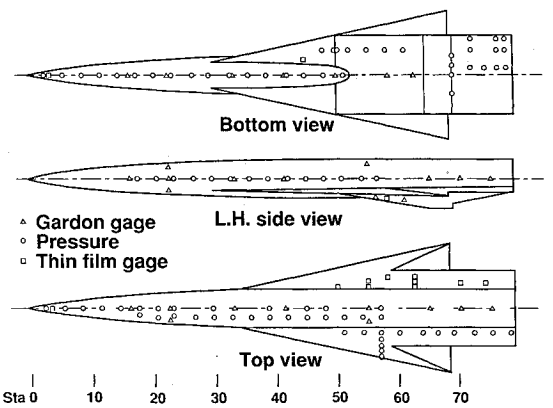

Fig. 1 Model pressure and heat-transfer instrumentation locations.

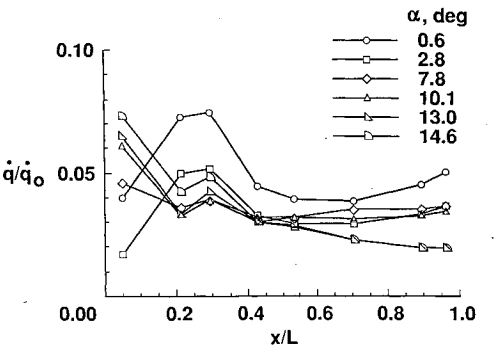

Fig. 2 Fuselage 0-deg ray heat transfer, $Re = 1.6 \times 10^6$/ft.

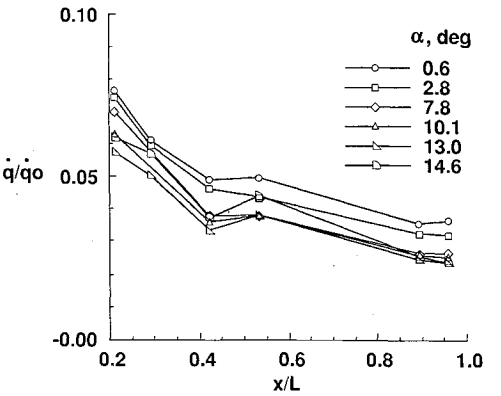

Fig. 3 Fuselage 90-deg ray heat transfer, $Re = 1.6 \times 10^6$/ft.

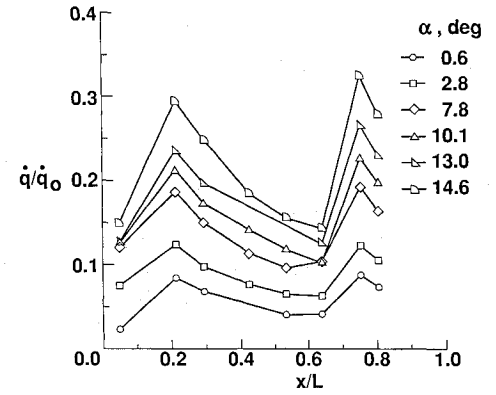

Fig. 4 Fuselage 180-deg ray heat transfer, $Re = 1.6 \times 10^6$/ft.

Results and Discussion

Heat Transfer Data

Anderson[4] has said, "Accurate experimental heat transfer data in hypersonics has always been a challenge to obtain, and calculations of the aerodynamic heating have been equally dif-

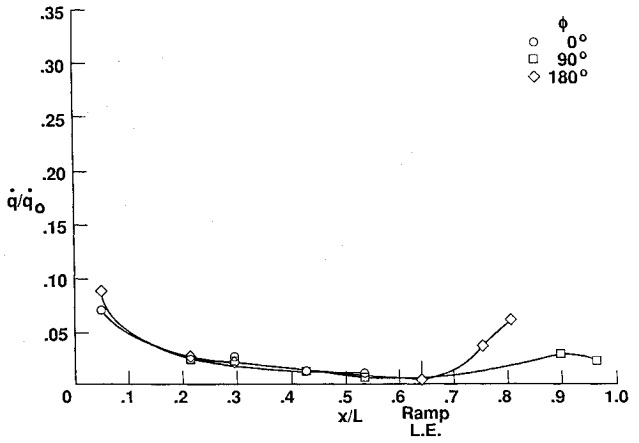

Fig. 5 Fuselage heat transfer, $\alpha = 0.5$ deg, $Re = 0.6 \times 10^6$/ft.

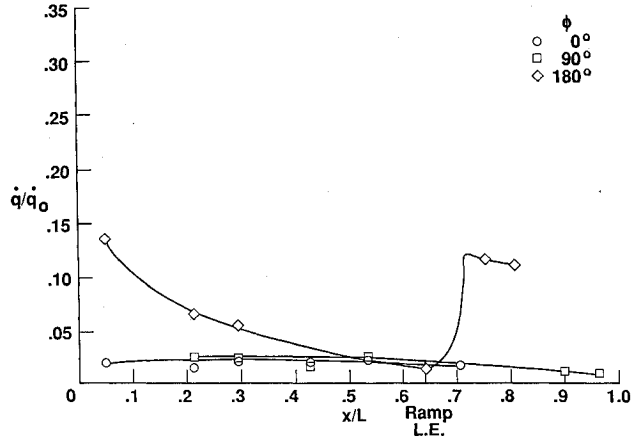

Fig 6 Fuselage heat transfer, $\alpha = 7.2$ deg, $Re = 0.6 \times 10^6$/ft.

ficult." With this in mind, the heat-transfer data will be presented first and no heat-transfer calculations will be shown.

Fuselage heat-transfer data (local heat transfer nondimensionalized by the stagnation heat transfer to a 1-ft, full-scale hemisphere at the particular test conditions—about 147 Btu/ft^2-s for the high Reynolds number test condition and about 103 Btu/ft^2-s for the low Reynolds number test condition) at the various angles of attack investigated for three circumferential angles ($\phi = 0$, 90, and 180 deg) at the high Reynolds number test condition are presented in Figs. 2–4. These data were all obtained with the boundary-layer trips installed (note that the first measurement in both the 0- and 180-deg rays was made upstream of the nose trip location) in order to insure turbulent flow over the model. For the most part, the results shown in these figures are what would be expected from classical hypersonic flow considerations. Comparison of the data at the lowest angle of attack shows that the heat-transfer rate at $\phi = 0$, 90, and 180 deg, with the exception of the compression ramp, is essentially the same at each of the stations around the fuselage (note that the y-axis scales are not the same for the three figures). The windward ray measurements made upstream of the trip location ($x/L = 0.058$) are somewhat lower than that downstream of the trips, which would indicate that the flow was laminar upstream of the trips. As the angle of attack was increased, the windward ray ($\phi = 180$ deg – Fig. 4) heat-transfer rates increased and the leeward rays ($\phi = 0$ deg – Fig. 2 and 90 deg – Fig. 3) remained relatively constant. Perhaps the most interesting finding from these data is that heat transfer on the leside at angle of attack is only slightly lower than that for the fuselage as a whole at 0 deg.

The heat-transfer data from the two low Reynolds number runs are presented in Figs. 5 and 6. The trend of heat transfer with angle of attack is the same as that for the high Reynolds number data. That is, the heat transfer is essentially the same at $\phi = 0$, 90, and 180 deg at the angle of attack of about 0 deg, whereas the windward ray ($\phi = 180$ deg) heat transfer increased at the higher angle of attack. Also, the leeward heat-transfer level is about the same at the higher angle of attack as for the 0-deg run. An indication that the flow was laminar over the whole fuselage is the fact that the heat-transfer rate decays with x/L from the first measurement location in the nose; whereas for the high Reynolds number runs, the heat transfer rate is low at the first measurement location and then rises after the trip location and decays from that value.

Wing Upper Surface Heat Transfer

Wing upper surface, heat-transfer data at the high Reynolds number test condition as a function of x/L for rows of thin film, heat-transfer gauges at three butt lines on the flat next to the fuselage (see Fig. 1 for location) are shown in Fig. 7. Like the leeside fuselage heat transfer, these data show a distribution for each of the three butt lines that do not change with angle of attack. (As with the leeside fuselage heat transfer, the levels for the angle of attack data are slightly below the 0-deg levels.) The butt line furthermost from the fuselage, ($y/b/2 = 0.490$) and, hence, closest to the edge of the flat, shows a lower level than the two inner rows. This would seem to indicate that the flow has started to experience three-dimensional effects at this butt line, whereas the inner two exhibit primarily two-dimensional flow characteristics. This conclusion is further strengthened when the data are plotted as a function of the distance from the wing leading edge rather than a function of x/L (not shown). Doing this shows that the two inner butt lines have very similar characteristics, whereas the outer is at a somewhat lower, constant level.

These same heat-transfer locations are plotted in Fig. 8 for the low Reynolds number test condition. Here it is seen that the variation for the three butt lines for both angles of attack is somewhat smaller for this untripped flow condition, than for the tripped flow condition of the previous figures. In addi-

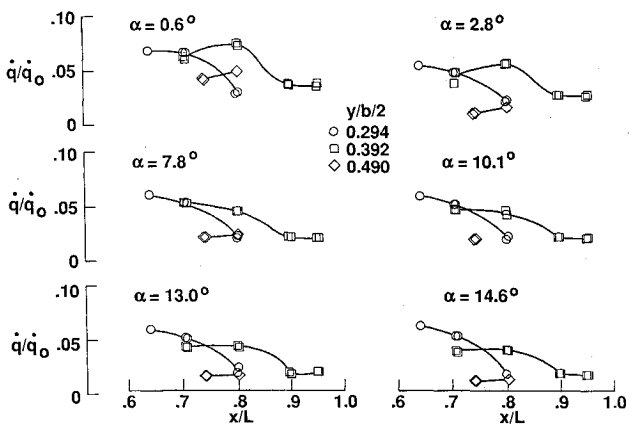

Fig. 7 Wing upper surface heat transfer, $Re = 1.6 \times 10^6$/ft.

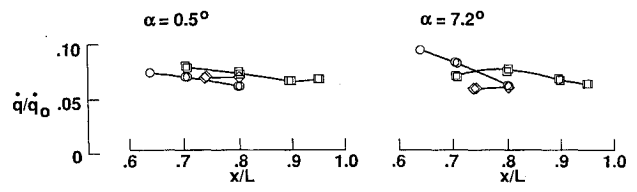

Fig. 8 Wing upper surface heat transfer, $Re = 0.6 \times 10^6$/ft.

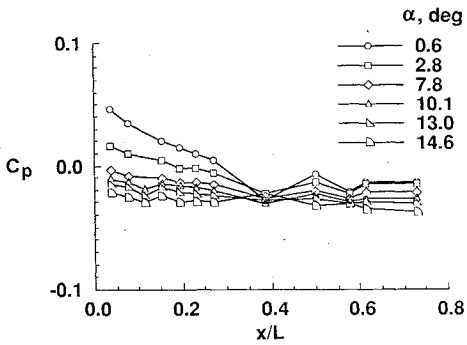

Fig. 9 Fuselage 0-deg ray pressure coefficients, $Re = 1.6 \times 10^6$/ft

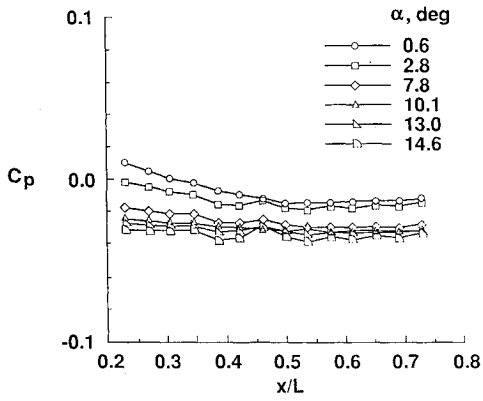

Fig. 10 Fuselage 30-deg ray pressure coefficients, $Re = 1.6 \times 10^6$/ft.

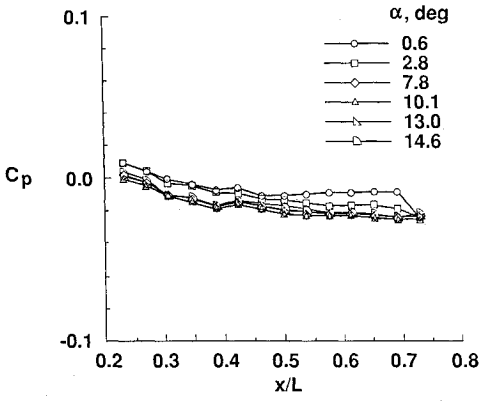

Fig. 11 Fuselage 90-deg ray pressure coefficients, $Re = 1.6 \times 10^6$/ft.

tion, when plotted as a function of distance from the leading edge (not shown), it was seen that the flow does not have quite the same two-dimensional characteristics as do the high Reynolds number data with the middle butt line row appearing to behave more like the outboard row than the inboard row.

Fuselage Pressure Coefficients

Fuselage pressure coefficients obtained for four longitudinal rays of orifices ($\phi = 0$, 30, 90, and 180 deg) at the high Reynolds number test condition (q_∞ averaged 9.891 psi for the high Reynolds number test condition and 4.094 psi for the low Reynolds number test condition) at the various angles of attack are shown in Figs. 9–12. As expected, and as with the heat transfer, the pressures are essentially constant around the body at the lowest angle of attack. The windward ray ($\phi = 180$ deg) exhibits an increase in pressure coefficient with angle of attack (also similar to the heat transfer) that can be best seen in Fig. 12, whereas the leeside pressure coefficients (see Fig. 9) move in the negative direction with angle of attack (although the magnitude of variation with angle of attack is much greater for the windward side than for the leeside). The discontinuities in the pressure coefficient distribution for the $\phi = 0$-deg pressures at stations 0.388 and 0.577 for the angles of attack of 0.6 deg and 2.8 deg (see Fig. 9) and for station 0.731 at $\phi = 90$ deg at the same two angles of attack are probably due to local irregularities in the model surface near these pressure orifices. The pressure coefficients from these orifices become much better behaved for the higher angles of attack investigated where the surface near the orifices would be shielded from the direct impact of the flow.

The fuselage pressure coefficients for the two low Reynolds number runs are not shown because they were very similar in appearance to the high Reynolds number data. This was expected because the pressure field is primarily an inviscid phenomena on which Reynolds number has only minor effects.

Data/Theory Comparison

With a limited amount of time available, it was decided to investigate a very classical technique for pressure prediction: modified Newtonian theory. The nose and forebody of the model were fit with the following curve so that the local slope could be easily calculated

$$r = 0.00010471 + 0.16137x - 0.0021344\,x^2$$

For the high Reynolds number test condition, the maximum pressure coefficient was calculated to be 1.825.

The results of the modified Newtonian predictions of the bottom row ($\phi = 180$ deg) pressure coefficients are presented in Fig. 12. The results are generally quite good. The worst case comparison is for the essentially 0-deg angle of attack case, which is not surprising because the theory is based on the flow impacting the surface and for this angle of attack the flow impacts the least.

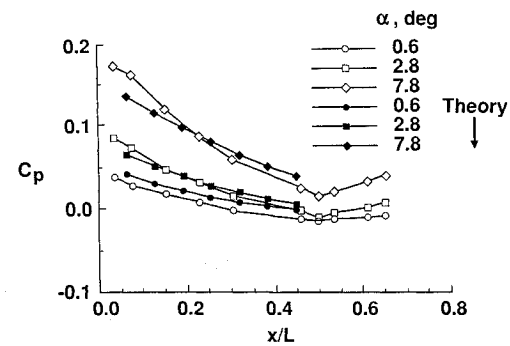

a) $\alpha = 0.6$, 2.8, and 7.8 deg

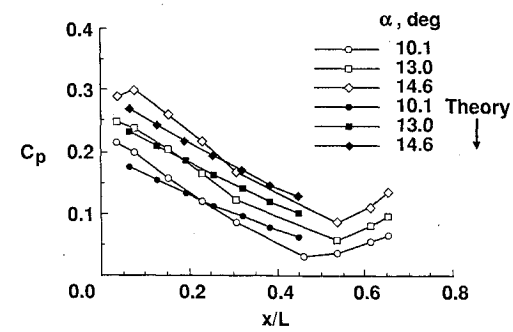

b) $\alpha = 10.1$, 13.0, and 14.6 deg

Fig. 12 Fuselage 180-deg ray pressure coefficients and comparison with modified Newtonian theory, $Re = 1.6 \times 10^6$/ft.

Concluding Remarks

An experimental investigation has been conducted in the NASA Langley 8′HTT to obtain pressure and heat-transfer data on a model of a hypersonic, wing-body configuration at a nominal Mach number of 6. This investigation provides a data base of pressure and heat-transfer data for a realistic configuration (with a concentration on the leeside of the vehicle) for use in the verification of computational techniques. In addition, a number of observations were made concerning the data.

1) The fuselage, windward side heat transfer increased with increasing angle of attack for both Reynolds number test conditions, as expected.

2) The fuselage, leeside heat transfer remained relatively constant at only slightly less than the respective 0 deg levels at all angles of attack for both Reynolds number test conditions.

3) At the high Reynolds number test condition, the wing upper surface heat transfer behaved much like the leeside of the fuselage. That is, the heat-transfer distribution was relatively constant with angle of attack at levels just slightly below that for 0 deg. Also, the character of the flow was primarily two dimensional for the instrumented area. The low Reynolds number test-condition data for these measurements show that the flow exhibits more three-dimensional characteristics.

4) Fuselage, windward side pressure coefficients, as with the heat transfer, increase with increasing angle of attack for both Reynolds number test conditions.

5) Fuselage, leeside pressure coefficients decrease slightly with angle of attack but remain relatively close to a value of 0 and indicate the inviscid character of the pressure dependence as opposed to the dependence of the heat transfer on the local state of the boundary layer.

6) Comparison of fuselage, windward side pressure coefficients with predictions from modified Newtonian theory show relatively good agreement.

References

[1]Howell, R. R., and Hunt, L. R., "Methane-Air Combustion Gases as an Aerodynamic Test Medium," *Journal of Spacecraft and Rockets*, Vol. 9, No. 1, 1972, pp. 7–12.

[2]Kelly, H. N., and Wieting, A. R., "Modification of NASA Langley 8-Foot High Temperature Tunnel to Provide a Unique National Research Facility for Hypersonic Air-Breathing Propulsion Systems," NASA TM-85783, May 1984.

[3]Reubush, D. E., Puster, R. L., and Kelly, H. N., "Modification to the Langley 8-Foot High Temperature Tunnel for Hypersonic Propulsion Testing," AIAA Paper 87-1887, June 1987.

[4]Anderson, J. D., Jr., "A Survey of Modern Research in Hypersonic Aerodynamics," AIAA Paper 84-1578, June 1984.